Eur. Phys. J. D **22**, 355–364 (2003)
DOI: 10.1140/epjd/e2003-00050-8

THE EUROPEAN PHYSICAL JOURNAL D

Investigation and characterization of a 3D double optical lattice

H. Ellmann[1,a], J. Jersblad[1], and A. Kastberg[2]

[1] Department of Physics, Stockholm University, 106 91 Stockholm, Sweden
[2] Department of Physics, Umeå University, 901 87 Umeå, Sweden

Received 5 September 2002 / Received in final form 16 December 2002
Published online 26 February 2003 –

Abstract. We present a detailed description of measurements performed with a novel double optical lattice setup. In this we trap two different cesium hyperfine ground states in separate periodic potentials. A detailed account of the technical solutions and its foundations are given. We demonstrate the possibility to modulate the relative spatial position of the lattices and perform a series of systematic measurements in order to investigate the static and dynamic properties of the double optical lattice system.

PACS. 32.80.Pj Optical cooling of atoms; trapping – 32.80.Qk Coherent control of atomic interactions with photons

1 Introduction

Optical lattices are periodic arrays of micro-traps created by the interference of two or more laser beams [1,2]. The potential depth of these traps is low, typically around a hundred recoil energies. One key feature of near-resonant optical lattices (NROL) is an inherent "Sisyphus" cooling mechanism that stems from the interplay between the dipole force and optical pumping in multilevel atoms. It is efficiency makes it possible to extract enough kinetic energy from the atoms so that they become localized in the optical potential wells. The atoms are thus arranged in a crystal-like ordered structure, kept in place only by their interaction with the radiation field, and are therefore well isolated from the environment. The interatomic distance is of the order of the optical wavelength, which is large enough to prevent the atoms from coupling *via* dipole-dipole interactions. If it is possible, however, to change the interatomic distances, these interactions could be turned on/off in a controlled way in order to entangle atomic wave functions. Thus, one essential prerequisite for the experimental implementation of quantum computational schemes would be fulfilled. Optical lattices have therefore been suggested as promising candidates to implement various schemes for coherent quantum state manipulations [3–6]. Most proposals rely on the idea of two interpenetrating optical lattices that trap two different quantum states. By changing the relative position of these lattices, interactions and, thus, phase-shifts in the atomic wavefunctions would be introduced. This can be used, for example, to build quantum-logic gates [3,5], simulate ferromagnetism or to generate spin-squeezing [5]. While many applications require high filling factors in the lattices, possibility to address single atoms, and that the atoms are brought to their motional ground states, some experiments can be performed with relaxed demands on occupation number, addressing and ground state occupancy.

Earlier suggestions for quantum state manipulations involving optical lattices rely on the well-known lin⊥lin configuration for one-dimensional optical lattices [1,2]. Here, two orthogonally polarized counterpropagating laser beams of equal irradiance and wavelength produce an interference pattern that can be decomposed into two standing waves of circular polarizations (σ_+ and σ_-), spatially offset by $\lambda/4$. Due to a negative light shift (which is the case for negative detuning), the nodes of these two standing waves become potential minima for two different spin directions. If the atoms are slow enough, they get trapped around these minima. By changing the angle between the polarization vectors, atoms with opposite spins can be brought together. In such a configuration, however, the atoms are confined in only one direction, so that spatial diffusion and many-body effects have to be accounted for. Furthermore, this scheme also alters the shape of the potential wells.

In this paper we summarize the results from [7] and present a more detailed account of the approach in which we use two three-dimensional optical lattices for Cs, using the D2 line. Apart from using the ordinary cycling transition ($F_g = 4 \rightarrow F_e = 5$)[1], we create an additional lattice based upon the ($F_g = 3 \rightarrow F_e = 4$) resonance,

[a] e-mail: ellmann@physto.se

[1] F is the total angular momentum quantum number.

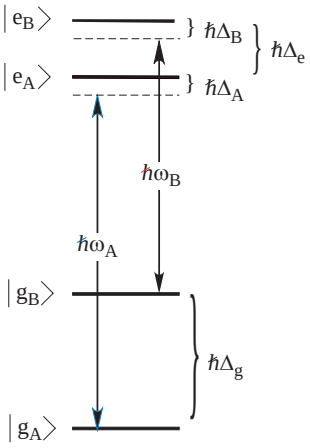

Fig. 1. Schematic level diagram. Two ground states $|g_A\rangle$ and $|g_B\rangle$, separated by $\hbar\Delta_g$, are connected by two laser fields of frequencies ω_A and ω_B to the excited states $|e_A\rangle$ and $|e_B\rangle$. The splitting between the excited levels is $\hbar\Delta_e$.

thus replacing the repumper beam of standard laser cooling schemes. Hence, two different Cs ground states are trapped in two distinct lattices with virtually no cross talk, but with nearly identical lattice constants. The lattices can be moved relative to each other along all three coordinate axes and qualifies as a candidate for quantum state manipulations.

2 Concept

Our idea is to use two different transitions to trap two different ground states $|g_A\rangle$ and $|g_B\rangle$ in two spatially overlapping lattices that are created by two distinct laser fields with frequencies ω_A and ω_B (see Fig. 1). The prerequisites are that on one hand the energy separation between the ground states $\hbar\Delta_g$ is large enough to avoid cross-talk between the respective lattices, but on the other hand so small that the lattice constants are practically identical. Thus, the lattices will not dephase significantly across the lattice volume (diameter L). These conditions can be summarized as follows:

$$\begin{aligned} \Delta_g &\gg \Delta_e \\ \Delta_g &\ll \frac{c}{L} \\ \Delta_g &\gg \Delta_A, \Delta_B. \end{aligned} \tag{1}$$

In our experiment, this scheme is applied to optical lattices operating on the D2 line in Cs ($\lambda \approx 852\,\mathrm{nm}$). Two diode lasers are detuned below the ($F_g = 4 \rightarrow F_e = 5$) and ($F_g = 3 \rightarrow F_e = 4$) transitions respectively, so that $\Delta_g/2\pi \approx 9.2$ GHz, $\Delta_e/2\pi \approx 250$ MHz and $L \approx 0.6$ mm. We use a four beam lattice geometry which is a generalization of the 1D lin⊥lin configuration to 3D [1,2]. Two pairs of laser beams with orthogonal polarization propagate in the xz-plane and yz-plane, respectively. The angle between the beams of each pair is 90°, and the angle between each beam and the vertical quantization axis is 45° (see the inset in Fig. 2). The resulting lattice structure is tetragonal, with alternating σ_+/σ_- sites that trap atoms in the magnetic substates $m_g = \pm F_g$. The lattice constants are $a_\perp = 2\lambda/\sqrt{2}$ perpendicular to the quantization axis, and $a_{||} = \lambda/\sqrt{2}$ parallel to the quantization axis.

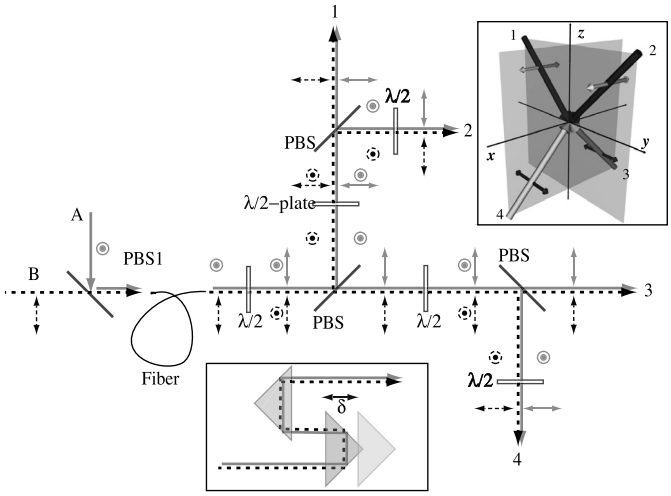

Fig. 2. Schematic overview over the alignment of the double optical lattice. Shown is, how the two different laser beams are overlapped and then split into four beams. The upper inset shows the geometrical beam configuration. In the lower inset, the principle of beam prolongation is illustrated.

A detailed treatment of the lattice properties is given in Appendix A.

The advantage of using $N + 1$ beams for an N-dimensional lattice is the robustness of the configuration against random phase changes in either one or all beams. As shown in Appendix A, a phase fluctuation occurring equally in all four beams of one lattice, *e.g.* caused by a random phase jump in a laser, will leave the lattice pattern unaltered. Consequently, there is no need to phase lock the two lasers that generate lattices A and B. Phase changes occurring in a single beam of one lattice will only translate the lattice. By letting the 2×4 beams that form the two lattices follow identical beam paths, and giving them identical spatial modes, such translations will happen equally in both lattices.

3 Implementation

In order to implement this concept, we use the setup shown schematically in Figure 2 for the alignment of the lattice beams. The two laser beams used to generate lattice A and B are combined with a polarizing beam splitter cube (PBS 1) and fed into an optical fiber for spatial filtering. Leaving the fiber, the beams overlap perfectly and have orthogonal polarizations. The polarizations are then rotated with a $\lambda/2$ plate in such a way that they form a 45° angle with the plane of incidence of another polarizing beam splitter. Thus, both beam A and beam B are split into two branches with equal irradiance for each frequency. Repeating this procedure for each branch, one gets a total number of four beam pairs, each containing two frequencies. This arrangement is very sensitive to impurities in the polarizations, which therefore have to be carefully cleaned. A slight error in polarization will make

it impossible to balance the irradiances of the different lattice beams.

In this way one can be sure that the relative position of the lattices is insensitive to phase fluctuations, caused for instance by micro-vibrations in optical components. Any vibration in an optical component in beam line A (or B) occurring before PBS 1 (see Fig. 2) will propagate in all four branches and will not have any effect on the lattices. On the other hand, if a small displacement occurs in a component on the other end of the fiber, both beams will be affected and the lattices will be translated equally. A large displacement (several millimeters), however, will translate the lattice by slightly different amounts. This opens up the possibility for a relative displacement, or a change in relative spatial phase, of the lattices. Such a large displacement can be achieved by changing the optical path length for the beam pairs with a low-cost device consisting of a pair of right angle prisms, one of which is mounted on a linear translation stage (see Fig. 2). The translation stages can be rotated so that their translation axes are parallel with the directions of the incoming beams. Moving the translation stage will thus not displace the beam, but only result in a prolongation (2δ) of the optical path length (and hence the relative phase of the beams). Such a "translator" is placed in each beam pair, which gave us the opportunity to apply relative phase changes in all directions. Prolonging beam 4 and shortening beam 3, for instance, results in a relative translation along the x-axis. Prolonging beams 3 and 4 by the same amount changes the spatial phase along the z-axis. In Appendix A we derive the needed translations for certain spatial phase shifts between the two lattices. The translation stages were operated manually.

4 Experimental details

The atoms are provided by a magneto-optical trap (MOT) initially tuned 2–3Γ below the ($F_\mathrm{g} = 4 \rightarrow F_\mathrm{e} = 5$) resonance. Here, Γ denotes the natural linewidth, with $\Gamma/2\pi = 5.2$ MHz. The MOT is loaded from a chirped-slowed atomic beam, produced in a thermal source. The loading takes about 4 s and fills the MOT with approx 6×10^6 atoms at a peak density of 1.7×10^{11} cm^{-3}. In order to avoid optical pumping into the dark $F_\mathrm{g} = 3$ ground state due to off-resonant excitations, we apply a repumper beam, tuned to the ($F_\mathrm{g} = 3 \rightarrow F_\mathrm{e} = 4$) resonance. The atomic cloud is further cooled in several time-steps in which the magnetic field of the MOT-coils is switched off, the detuning is increased and the irradiance reduced. Eventually, the MOT beams are switched off and the lattice beams are turned on. We let the atoms equilibrate for about 25 ms before the lattice beams are extinguished and we extract the thermal velocity distribution along the (vertical) quantization axis from a time-resolved fluorescence signal, the so-called time-of-flight (TOF) method [8]. As the TOF probe we use a thin sheet of light (about 1 cm wide, less than 50 μm thick, and located 5 cm below the optical lattice) is produced with a cylindrical lens ($f = 1$ m) and contains two frequencies, resonant to the ($F_\mathrm{g} = 3 \rightarrow F_\mathrm{e} = 4$) (probe A) and ($F_\mathrm{g} = 4 \rightarrow F_\mathrm{e} = 5$) (probe B) transitions. Analogous to the lattice beams, they are combined before they are fed through an optical fiber for spatial filtering. Our combined velocity resolution is around 0.05 mm/s, where the main contribution is fluctuations in the width of the atomic cloud (approx. 0.4 mm in diameter, with fluctuations significantly smaller than 10%), which has to be deconvoluted from the data. The probe beam is so thin that is does not contribute to the error in the temperature measurements, and neither does the pointing stability or the electronic time resolution of the detection. When assigning a temperature to a velocity distribution, the main error probably stems from the fact that the distribution does not necessarily need to be Gaussian. We estimate that the total error in the absolute value of the temperature is about 50 nK, as long as the Gaussian fits are reasonable. When comparing two different measurements, we can see temperature differences smaller than that.

5 Temperature measurements

In order to test the scheme to shift the optical lattices, and to see if a double optical lattice would lead to improved cooling, we measured the equilibrium temperature T_B of the atoms trapped in the ($F_\mathrm{g} = 4$) ground state (lattice B) as a function of the relative lattice displacement. Both lattices were operated 19Γ below their respective resonances. We displaced the lattices along one coordinate axis by changing the position of the translation stages, as described above, and we used probe B for the TOF measurements. We define the relative spatial phases

$$\varphi_{x,y} = 2\pi\frac{\delta_{x,y}}{a_\perp}, \qquad \varphi_z = 2\pi\frac{\delta_z}{a_\parallel}$$

where δ_i is the shortest distance between a σ_+-site of lattice A and a σ_+-site of lattice B projected on the i-coordinate. In Figure 3a [7] the result of a scan along $\hat{\mathbf{z}}$ for fixed $\varphi_{x,y}$ is shown, where the temperature T is plotted *versus* the relative displacement δ_z in units of the lattice constant $a_\parallel$. The origin is arbitrary and corresponds to an equal displacement of all four translation stages. There is a clear dependence of T on δ_z. As shown in Figure 3b, the modulation amplitude of the sinusoidal curves decreases when lattice A is close to the ($F_\mathrm{g} = 3 \rightarrow F_\mathrm{e} = 4$) resonance, while the minimum temperature remains constant. A notable exception occurs when $\Delta_\mathrm{A} = 0\Gamma$, where the minimum temperature is slightly lower. compared to an ordinary optical lattice with a single resonant repumping beam. The periodicity of all fits is $0.9a_\parallel$ which within the experimental uncertainties reproduces the calculated value $a_\parallel$.

In order to explain the variation of T with δ_z one has to distinguish between two cases. If lattice A is operated close to resonance, $\Delta_\mathrm{A} \ll \Gamma$, the modulation depth of the optical potential is very small. For this case, a model introduced in [9] can be applied. Here, the optical potential for the lower ground state is not modulated, but exhibits

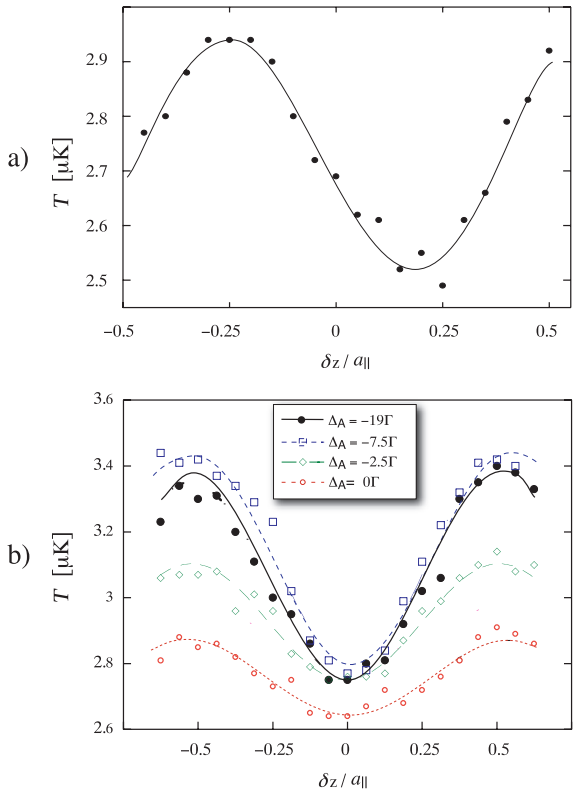

Fig. 3. (a) Temperature as a function of relative displacement δ_z of the two lattices in units of the lattice constant $a_{\|}$ (from [7]). (b) The same for different detunings Δ_A. Each data point is an average of 5 TOF measurements. Also shown are fits of the form $T = T_0 + C\,\sin(2\pi z/q)$.

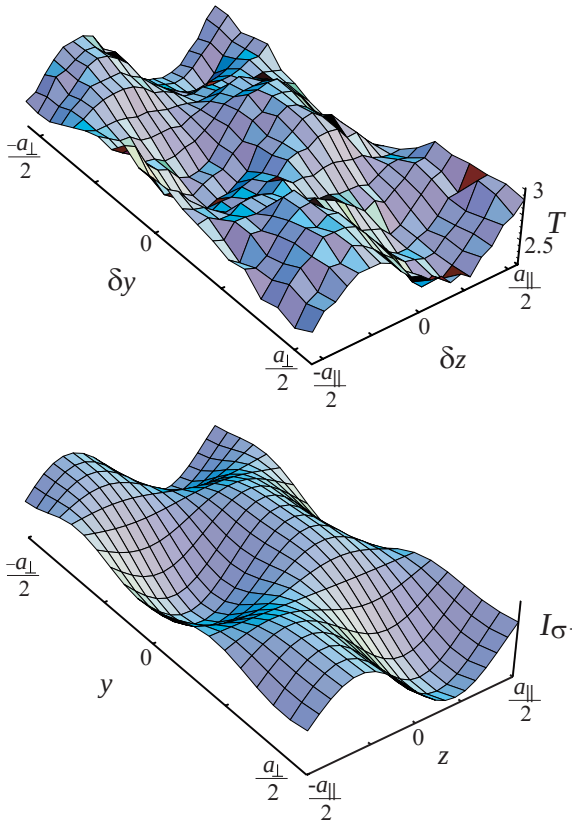

Fig. 4. (a) Measured temperature in the double optical lattice plotted as a function of the relative displacements δ_y, δ_z of the two lattices in the yz-plane (from [7]). (b) Calculated irradiance (in arbitrary units) of the σ_+ component as a function of position for one of the lattices.

a polarization gradient. If σ_+-sites of the optical lattice overlap with σ_+-sites of the repumping light, cooling is enhanced, while σ_+-sites overlapping with σ_--sites lead to heating.

For higher modulation depths, the variation can be explained with another, similar, semi-classical picture in which the atoms perform oscillating motion in the wells of the adiabatic potentials [7]. If the σ_+-sites of one lattice coincide with the σ_+-sites of the other, optical pumping will transfer the atoms from one trapping potential to another and nothing much will happen. On the other hand, if σ_+-sites overlap with σ_--sites (and *vice versa*) optical pumping will now move the atom from a trapping potential to an antitrapping one. The gain in potential energy from the light field is converted into kinetic energy as the atom starts to slide down the potential. Additional heating occurs due to multiple optical pumping cycles because in the new ground state it "sees" σ_--light. We therefore expect that temperature minima correspond to $\varphi_z = 0$, whereas maxima occur for $\varphi_z = \pi$.

We also performed a two-dimensional scan across the the yz-plane [7]. First a T *vs.* δ_x-scan was made to determine a temperature minimum. Thus we made sure the lattices overlapped with respect to a projection onto the x-direction. We then repeatedly took T *vs.* δ_z-curves for various δ_y. This could be used to construct a temperature surface for the selected plane, as illustrated in Figure 4a. Also shown is a plot of the calculated irradiance of the σ_+-component of the laser field, which corresponds to the diabatic optical potential [1,2] for the $|F_g = 4, m_g = +4\rangle$ ground state. A comparison shows that the dependence of the temperature on the relative displacement between the lattices allows us to create a map of the potential topography.

Furthermore we varied the potential depth in lattice A or lattice B, $U_{A,B}$, for given pairs of detuning $\Delta_{A,B}$ and measured T_B using only probe B. The results are shown in Figure 5. The plots are very similar, with the linear dependence of T_B on U and the abrupt increase of the temperature for low U. The slope $dT_B/dU_B = 0.013\ \mu K/E_R$ [2] is in good agreement with previous results [10]. The measured value for dT_B/dU_A is 0.006 $\mu K/E_R$. In order to emphasize this small slope, Figure 5a is plotted in a different scale than Figure 5b. For broad distributions, we are more sensitive to fluctuating backgrounds, and thus the scatter in the data is slightly larger lager (around 100 nK) than for lower temperatures.

[2] E_R is the recoil energy defined as $E_R = (\hbar k)^2/2m$, where $k = 2\pi/\lambda$ and m is the atomic mass.

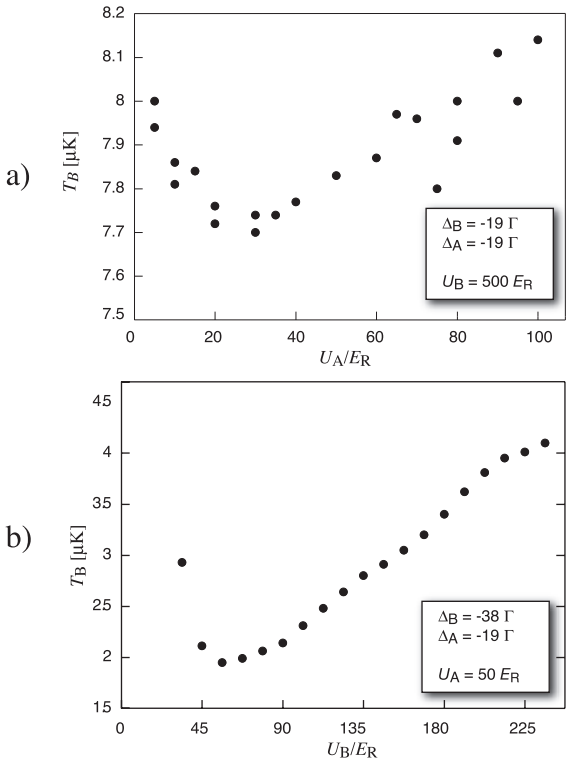

Fig. 5. Temperature of atoms in lattice B as a function of the modulation depths $U_{A,B}$. (a) T_B scales linearly with U_A for depths down to $30E_R$. At lower modulation depths the temperature increases again. (b) T_B plotted *versus* U_B.

The result in Figure 5 could indicate that Sisyphus cooling is present in lattice A, but a more systematic investigation would be necessary to confirm this hypothesis.

6 Rate measurements

An important difference between the two lattices is that one of them is operating on the cycling ($F_g = 4 \rightarrow F_e = 5$) transition, while the other lattice uses the non-cycling ($F_g = 3 \rightarrow F_e = 4$) transition. We therefore expect that the relative populations of the two lattices are highly asymmetric, because the atoms tend to become optically pumped into lattice B. The suggestions for coherent quantum state manipulation presented in [3–5] rely on controlled interactions between atoms of neighbouring lattice sites, where the interatomic distance is adjusted to induce phase shifts in the atomic wave functions. It is therefore important that both lattices are sufficiently populated so that induced collisions are probable. Also, the experiments have to be performed on a timescale smaller than the typical decoherence time. We have measured the relative number of trapped atoms in the lattices and the optical pumping rates between them. By switching off lattice A before lattice B for various time delays δt, lattice B is depleted. The relative number of atoms remaining in lattice B, N_B, is determined by integrating the area under

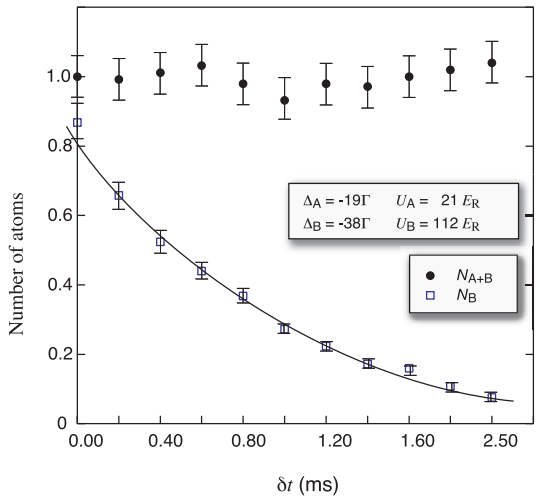

Fig. 6. Number of atoms in lattice B (normalized to N_{A+B}) and total number of atoms as a function of the time delay δt between the switching off lattice A and lattice B. Shown is also an exponential fit to the decay curve of N_B, yielding a decay time $\tau_B = 0.8$ ms.

the TOF signal when only probe B is used. The total number of atoms N_{A+B} is obtained using both probe A and probe B simultaneously. In this case probe A will pump atoms from $|g_A\rangle$ into $|g_B\rangle$ where they can be detected with probe B. Figure 6 shows a typical plot for an optical pumping curve taken at $\Delta_A = -19\Gamma$, $U_A = 21E_R$, $\Delta_B = -38\Gamma$, $U_B = 112E_R$[3]. N_B decays exponentially with increasing delay time, while N_{A+B} remains constant. Slight irregularities in N_{A+B} can be attributed to run-to-run fluctuations when loading the MOT. To test the reliability of the method described above we measured N_B as a function of δt using an absorption imaging technique. The results were identical within the experimental uncertainty.

We performed a systematic investigation of both pumping rate and relative populations for a wide range of the lattice parameters [7], with Δ_A ranging between -7.6Γ and -85Γ, and Δ_B between -7.7Γ and -38Γ. For each combination of detunings the decay rates were measured for beam irradiances from $I_{A,B} = 0.8$ mW/cm^2 to $I_{A,B} = 4.0$ mW/cm^2. An exponential was fitted to each decay curve from which the lifetime τ_B for the atoms in lattice B was extracted. In Figure 7a we show $\gamma_B = 1/\tau_B$ as a function of I_B for different detunings.

The optical pumping rate, γ_B, out of $|g_B\rangle$ increases with increasing irradiance, since the photon scattering scales linearly with the irradiance. The measured optical pumping times, τ_B, range between 0.6 ms and 4 ms, with an uncertainty of about 15–20%. We also notice that

[3] At large detunings, such as -38Γ, the laser frequency is actually closer to the next neighbouring transition. Nevertheless, U_B can still be calculated without taking this transition into account. This is because the atomic dynamics is dominated by the lowest of the total adiabatic potentials, which is in turn almost unaffected of the close blue detuned transition. This is shown experimentally in [10].

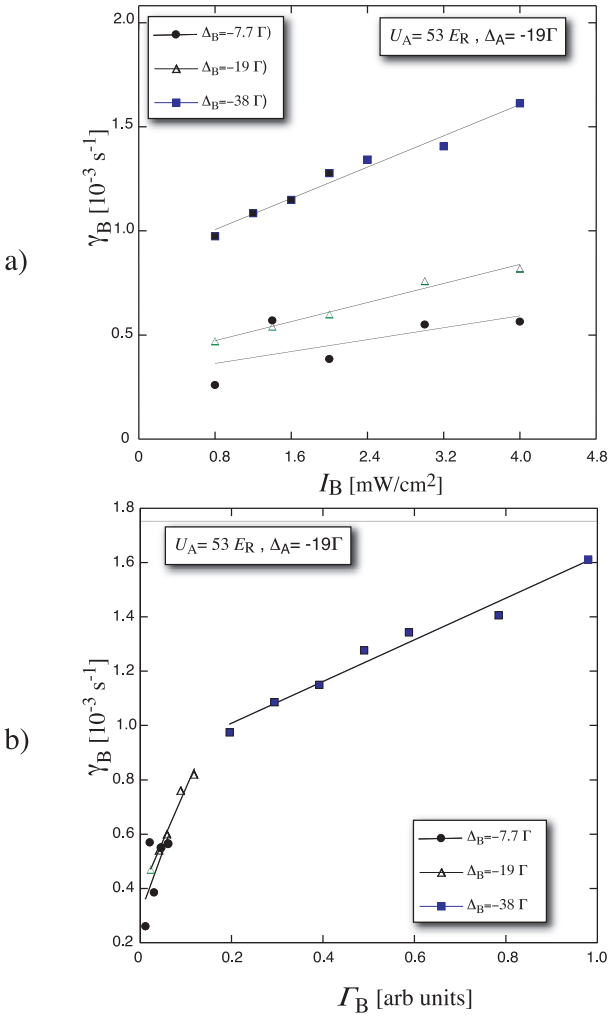

Fig. 7. (a) Optical pumping rates γ_B as a function of the irradiance I_B for three different detunings Δ_B. (b) The same data replotted as a function of the scattering rate Γ_B, which we define as irradiance divided by the square of the detuning with respect to the ($F_g = 4 \rightarrow F_e = 4$) transition. The insets show the parameters for the linear fits applied to the data points.

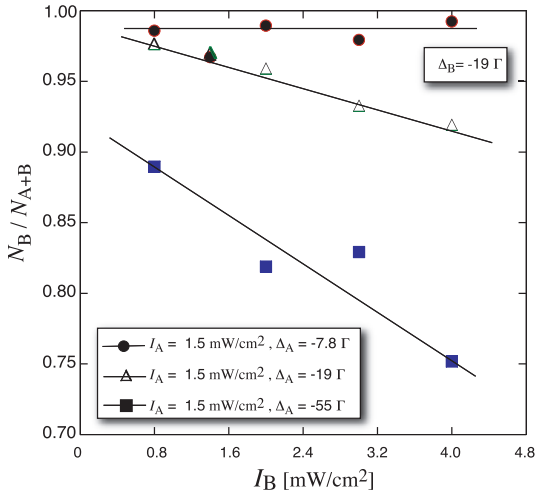

Fig. 8. Relative population of lattice B as a function of I_B for three different detunings of lattice A.

γ_B increases for increasing $|\Delta_B|$. This is explained by taking the non-cycling ($F_g = 4 \rightarrow F_e = 4$) transition into account. The detuning with respect to that transition is $\Delta_B + 48\Gamma$, so increasing $|\Delta_B|$ decreases the detuning to the non-cycling transition. For γ_B this is the relevant detuning, since excitation to $F_e = 4$ is the only path to $F_g = 3$. Hence optical pumping into $|g_A\rangle$ is enhanced. The linear fits to the data points do not intercept the origin, contrary to what one would expect.

In Figure 7b we replot the decay rates as a function of the scattering rate Γ_B, which we define as the departure rate out of lattice B due to the coupling between $F_g = 4$ and $F_e = 4$. Γ_B provides no universal scaling, indicating that the processes involved in transferring the atoms between the lattices are more subtle.

The optical pumping rate out of lattice A, γ_A, was estimated by assuming a trivial rate equation at steady state:

$$\frac{dN_B}{dt} = -\gamma_B N_B + \gamma_A N_A = 0. \quad (2)$$

This yields optical pumping times τ_A roughly between 6 μs and 300 μs, but with large error bars (around 50%).

For the measurements of the equilibrium populations, N_B and N_A, the same set of irradiances and detunings were used. As expected, the relative population of the $F_g = 4$ ground state is much larger than the population of $F_g = 3$. Typically $N_B/N_{A+B} \approx 95\%$. This number decreases with increasing (decreasing) irradiance in lattice B (lattice A), as shown in Figure 8. Also N_B/N_{A+B} decreases with increasing $|\Delta_B|$ due to off-resonant coupling from $F_g = 4$ to $F_e = 4$, and increasing $|\Delta_A|$ due to lower scattering rates (Fig. 8). For a set of detunings $\Delta_A = -55\Gamma, \Delta_B = -19\Gamma$ and optical potentials $U_A = 20E_R, U_B = 450E_R$, the relative population in lattice B was as low as 75%.

7 Discussion of the results

We find, that the temperature in a double optical lattice depends on the relative displacements δ_x, δ_y and δ_z. The modulation of the temperature is present for all investigated detunings Δ_A, although the mechanisms leading to the modulation might be different. The variation of the temperature in lattice B, T_B, with the optical potential in lattice A, is difficult to explain. The data was taken at high irradiances and at a detuning $\Delta_B = -19\Gamma$, so that it is possible, that atoms spend enough time in lattice A in order to be cooled. On the other hand, this would imply, that the temperature in a double optical lattice should be lower than in a single optical lattice, but our measurements indicate that this is not the case.

The pumping rates are, as expected asymmetric: lattice A is depopulated much faster than lattice B.

By adjusting irradiances and detunings one can manipulate these, and the relative populations, considerably. The departure rate out of lattice B, γ_B, is not a linear function of the optical pumping rate due to the ($F_g = 4 \rightarrow F_e = 4$) transition. Depending on the lattice parameters, the atoms are in very different regimes and optical pumping might be suppressed by the Lamb-Dicke effect. The optical pumping rates are small enough to keep the vibrational levels in the potential wells resolved [7].

At present, the model for the cooling and transfer processes in the double optical lattice is not complete. In the near future we plan to do numerical simulations, which hopefully will give us more insight.

8 Possible application for coherent quantum manipulations

In order to implement many of the suggestions in [3–5], several prerequisites have to be fulfilled.

Both lattices have to be sufficiently populated to allow controlled interactions. Our results show that it is possible to trap atoms in two different ground states and by choosing the lattice parameters (detunings, irradiances) appropriately, a significant amount of atoms will be in the lower ground state $|g_A\rangle$. At present, the filling factor of our optical lattices is around one percent, but this can be improved by loading from a compressed MOT [11]. Since [11] relates to optical lattices tuned far from resonance, we can not expect as high filling factor as in that work, but preliminary experiments show that our current occupation can be improved significantly. Furthermore, it is possible to transfer atoms between the lattices by stimulated Raman-transitions.

Although not always necessary [5], it is desirable that the atoms are in the vibrational ground states of their trapping potentials. Our double optical lattice offers the possibility for a new method for Raman sideband cooling which may facilitate this. This is described in [7].

The interactions between the atoms have to be switched on and off, on a time scale faster than the decoherence time. As shown in [12], a tightly bound atom in an optical lattice has a decoherence time of about 50 scattering times (τ_{sc}). If the mission is to build a quantum gate, and the q-bit is encoded in the internal state (lattice A or B), the optical pumping time between the lattices will be a more severe limitation. In our case, the optical pumping time out of lattice A is $1.7\tau_{sc}$ (given by the branching ratio from the upper level in the open transition). For lattice B, it depends on the detuning, but it is always much longer. This would require a gate time of less than a millisecond, even for the most favorable parameters among those we have used in this work. The system is still feasible, even at these near-resonance conditions, for more crude forms of quantum state manipulation, such as the simplest suggestions in [3], where not much time is needed. With more powerful lasers, the detuning could be increased substantially. If one set of lattice beams is detuned above its transition, and the other one below, one could use detunings as large as 5 GHz (resulting in a detuning of 14 GHz for the "unwanted" transitions). For a well depth of $100E_R$ the optical pumping time from lattice A would then be 3 ms, and a quantum gate at that speed may be possible.

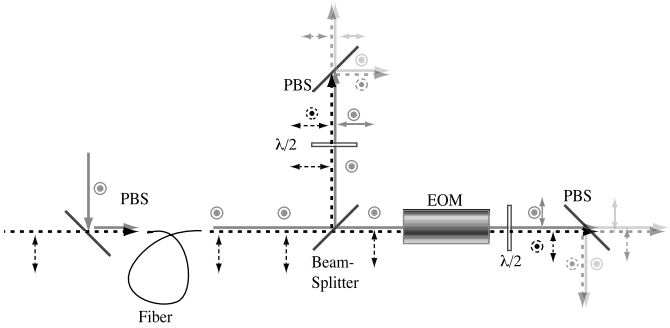

Fig. 9. Schematic overview of a setup involving an electro-optic modulator (EOM) as a phase shifter. After the fiber, the beams are split with a beam splitter, thus preserving the perpendicular polarizations of the two lattice frequencies. The EOM only shifts the phase of one polarization component.

If a q-bit is encoded in the motional state of a potential well, as recently suggested in [13], the situation changes. The wells for lattice A and B can easily be chosen to have the same curvature. For two overlapping lattices, one would get a situation analogous to two coupled quantum mechanical harmonical oscillators, both coupled to a thermal reservoir (compare [14] and [15]). In this situation, it is likely that the coherence of the motion is preserved as long as around $50\tau_{sc}$, as in [12]. On the other hand, displacements of the lattices will degrade this coherence, so "gating" can not work in quite the same way. If, on the other hand, a truly far-off resonance conditions is chosen one need not worry about optical pumping. One would then have mixed potentials, but it would still be possible to prepare specific motional states, and to do translations. This system would be similar to arrays of microtraps, reported about in [16], and to suggestions in [13]. The differences are that our lattice spacing is much smaller, which makes fast displacements easier, but single-bit addressing much harder. Also, we never have more than one atom per well, and typically much less, whereas in [16], they normally have several.

Relative displacements of the lattice have to be adiabatic with respect to the oscillatory motion of the atoms in the potential wells. The oscillation frequency is

$$\nu = \nu_R \sqrt{2U_0/E_R} \tag{3}$$

where U_0 is the modulation depth of the optical potential, and $\nu_R = E_R/h = 2.07$ kHz is the recoil frequency. With higher detunings and higher intensities, U_0 could be made large enough to yield frequencies higher than 100 kHz while maintaining low scattering rates. In the present setup, relative displacements are achieved by changing the optical path lengths with linear translation stages. To make rapid displacements possible we suggest the following scheme, illustrated schematically in Figure 9. The polarizing beam splitter (PBS) after the optical fiber from

Figure 2 is replaced with a non polarizing one, so that both light components remain orthogonally polarized. One of the two laser beam pairs passes a phase-shifting electro-optical modulator (EOM), which only shifts the phase of the horizontally polarized component. The polarization of the laser beams is rotated with a $\lambda/2$-plate to form a 45° angle with the next PBS. The splitting into four beam pairs is done in the same way as in Figure 2. In this way, a rapid relative displacement of the lattices is possible along the z-axis. Typical rise times for an EOM are in the order of 1 μs and below. The scheme can be further extended to allow a translation along all three Cartesian axis.

An alternative way to induce interactions could be to switch off the short-lived lattice A and move lattice B on a time scale short enough to avoid spatial diffusion of atoms in $|g_A\rangle$.

9 Conclusion

In summary, we have demonstrated that the suggested method to cool and trap two different cesium hyperfine ground state works, and that it is possible to modulate the relative position of the lattices, with the temperature as an indicator. In this paper we have described the methodology for doing double optical lattice experiments. We have also performed a detailed study of the transfer rates between the two lattices, which can be controlled by an appropriate choice of irradiances and detunings. The parameter space is large, and presently we have no consistent model to explain all the numerous results in a satisfactory way, but we hope to be able to clarify some of the open questions using numerical simulations.

We would like to thank Dr. Uwe Sterr for helpful discussions and Rafael Velasco-Fuentes for his help during the preparations of the experiment. This work was supported by Carl Tryggers Foundation and Knut and Alice Wallenbergs Foundation.

Appendix A

Electric field configuration

Comparing with Figure 2 the electric fields of the four laser beams constituting one optical lattice, can be written as:

$$\begin{aligned}\mathbf{E}_1 &= E_0\hat{\mathbf{x}}\cos(k_\perp y - k_\parallel z - \omega t)\\ \mathbf{E}_2 &= E_0\hat{\mathbf{x}}\cos(-k_\perp y - k_\parallel z - \omega t)\\ \mathbf{E}_3 &= E_0\hat{\mathbf{y}}\cos(k_\perp x + k_\parallel z - \omega t)\\ \mathbf{E}_4 &= E_0\hat{\mathbf{y}}\cos(-k_\perp x + k_\parallel z - \omega t),\end{aligned} \tag{4}$$

where $k_\perp = k_\mathrm{L}\sin\theta$ and $k_{||} = k_\mathrm{L}\cos\theta$, $k_\mathrm{L} = 2\pi/\lambda$, θ is the angle between the beams and the quantization (z-) axis and λ is the laser wavelength.

The total electric field can be computed (see *e.g.* [17]) in complex notation [18], and is a sum of two components with σ_+- and σ_--polarization respectively.

$$\begin{aligned}&\tilde{\mathbf{E}}_\mathrm{TOT} =\\ &2E_0\left\{\mathrm{e}^{\mathrm{i}\frac{\pi}{4}}\ \cos(k_\parallel z)\left(\frac{\cos(k_\perp y)+\cos(k_\perp x)}{2}\right)\right.\\ &\quad\left.+\ \mathrm{e}^{\mathrm{i}\frac{3}{4}\pi}\ \sin(k_\parallel z)\ \left(\frac{\cos(k_\perp y)-\cos(k_\perp x)}{2}\right)\right\}\ \mathrm{e}^{\mathrm{i}\omega t}\\ &+2E_0\left\{\mathrm{e}^{-\mathrm{i}\frac{\pi}{4}}\cos(k_\parallel z)\ \left(\frac{\cos(k_\perp y)-\cos(k_\perp x)}{2}\right)\right.\\ &\quad\left.+\ \mathrm{e}^{-\mathrm{i}\frac{3}{4}\pi}\ \sin(k_\parallel z)\left(\frac{\cos(k_\perp y)+\cos(k_\perp x)}{2}\right)\right\}\mathrm{e}^{-\mathrm{i}\omega t}.\end{aligned} \tag{5}$$

For $z = 0$ the lattice structure in the xy-plane is reduced to:

$$\begin{aligned}\tilde{\mathbf{E}}_\mathrm{TOT} &= 2E_0\left\{\mathrm{e}^{\mathrm{i}\frac{\pi}{4}}\left(\frac{\cos(k_\perp y)+\cos(k_\perp x)}{2}\right)\right\}\mathrm{e}^{\mathrm{i}\omega t}\\ &\quad+2E_0\left\{\mathrm{e}^{-\mathrm{i}\frac{\pi}{4}}\left(\frac{\cos(k_\perp y)-\cos(k_\perp x)}{2}\right)\right\}\mathrm{e}^{-\mathrm{i}\omega t}.\end{aligned} \tag{6}$$

In this plane the lattice constants are equal $a_\perp = 2\pi/k_\perp$. Along the z-axis ($x = y = 0$) the interference pattern can be written as:

$$\tilde{\mathbf{E}}_\mathrm{TOT} = 2E_0\left\{\mathrm{e}^{\mathrm{i}\frac{\pi}{4}}\ \cos(k_\parallel z)\ \mathrm{e}^{\mathrm{i}\omega t} + \mathrm{e}^{-\mathrm{i}\frac{3}{4}\pi}\ \sin(k_\parallel z)\ \mathrm{e}^{-\mathrm{i}\omega t}\right\}. \tag{7}$$

The lattice constant is $a_{||} = \pi/k_\perp$. The lattice structure is tetragonal, with alternating σ_+ and σ_- potential minima. In our experiment $\theta = 45°$, thus $k_\parallel = k_L\sin\theta = (1/\sqrt{2})k_L$, and $k_\perp = k_L\cos\theta = (1/\sqrt{2})k_L$. This particular configuration has a lattice constant $a_\parallel$ along the z-axis given by:

$$a_\parallel = \frac{\pi}{k_\parallel} = \frac{\pi}{\frac{1}{\sqrt{2}}k_L} = \frac{1}{\sqrt{2}}\,\lambda \tag{8}$$

and in the x and y-axis the lattice constant is given by

$$a_\perp = \frac{2\pi}{k_\perp} = \frac{2\pi}{\frac{1}{\sqrt{2}}k_L} = \frac{2}{\sqrt{2}}\,\lambda. \tag{9}$$

Changing the optical path length for one beam

If the optical path length of beam 1 (see Fig. 2) is changed by a distance 2δ, the electric field $\mathbf{E}_1$ becomes:

$$\begin{aligned}\mathbf{E}_1 &= E_0\hat{\mathbf{x}}\cos(k_\perp y - k_\parallel z + 2\delta k_L - \omega t)\\ &= E_0\hat{\mathbf{x}}\cos(k_\perp y - k_\parallel z + \varphi - \omega t)\end{aligned} \tag{10}$$

here $\varphi = 2\delta k_L$ is the corresponding phase shift. Once more writing the total electric field as a phasor in a circularly polarized basis and repeating the transformation from the

$$\begin{aligned}\tilde{\mathbf{E}}_{\mathrm{TOT}} &= E_0\left\{\mathrm{e}^{-\mathrm{i}k_\parallel z}\mathrm{e}^{\mathrm{i}\frac{\varphi}{2}}\cos(k_\perp y+\varphi/2)+\mathrm{i}\mathrm{e}^{\mathrm{i}k_\parallel z}\cos(k_\perp x)\right\}\mathrm{e}^{-\mathrm{i}\omega t}+E_0\left\{\mathrm{e}^{\mathrm{i}k_\parallel z}\mathrm{e}^{-\mathrm{i}\frac{\varphi}{2}}\cos(k_\perp y+\varphi/2)+\mathrm{i}\mathrm{e}^{-\mathrm{i}k_\parallel z}\cos(k_\perp x)\right\}\mathrm{e}^{\mathrm{i}\omega t}\\ &= E_0\left\{\mathrm{e}^{-\mathrm{i}(k_\parallel z-\frac{\varphi}{4})}\cos(k_\perp y+\varphi/2)+\mathrm{i}\mathrm{e}^{\mathrm{i}(k_\parallel z-\frac{\varphi}{4})}\cos(k_\perp x)\right\}\mathrm{e}^{\mathrm{i}\frac{\varphi}{4}}\mathrm{e}^{-\mathrm{i}\omega t}\\ &\quad+E_0\left\{\mathrm{e}^{\mathrm{i}(k_\parallel z-\frac{\varphi}{4})}\cos(k_\perp y+\varphi/2)+\mathrm{i}\mathrm{e}^{-\mathrm{i}(k_\parallel z-\frac{\varphi}{4})}\cos(k_\perp x)\right\}\mathrm{e}^{-\mathrm{i}\frac{\varphi}{4}}\mathrm{e}^{\mathrm{i}\omega t}\end{aligned}\tag{11}$$

$$\begin{aligned}&\tilde{\mathbf{E}}_{\mathrm{TOT}}=\\ &2E_0\left\{\mathrm{e}^{-\mathrm{i}\frac{\pi}{4}}\cos(k_\parallel z-\frac{\varphi}{4})\left(\frac{\cos(k_\perp y+\varphi/2)-\cos(k_\perp x)}{2}\right)+\mathrm{e}^{-\mathrm{i}\frac{3}{4}\pi}\sin(k_\parallel z-\frac{\varphi}{4})\left(\frac{\cos(k_\perp y+\varphi/2)+\cos(k_\perp x)}{2}\right)\right\}\mathrm{e}^{-\mathrm{i}(\omega t-\frac{\varphi}{4})}\\ &+2E_0\left\{\mathrm{e}^{\mathrm{i}\frac{\pi}{4}}\cos(k_\parallel z-\frac{\varphi}{4})\left(\frac{\cos(k_\perp y+\varphi/2)+\cos(k_\perp x)}{2}\right)+\mathrm{e}^{\mathrm{i}\frac{3}{4}\pi}\sin(k_\parallel z-\frac{\varphi}{4})\left(\frac{\cos(k_\perp y+\varphi/2)-\cos(k_\perp x)}{2}\right)\right\}\mathrm{e}^{\mathrm{i}(\omega t-\frac{\varphi}{4})}\end{aligned}\tag{12}$$

preceding section we obtain:

see equation (11) above.

Equation (5), and equation (11) are equivalent under a change of variables $k_\parallel z \to (k_\parallel z - \varphi/4)$ and $k_\perp y \to (k_\perp y + \varphi/2)$. We thus obtain (after shifting the origin along the z-axis)

see equation (12) above.

A prolongation of the optical path of beam 1 with 2δ will thus lead to a phase change of the lattice by $\varphi/2$ along the y-axis and by $\varphi/4$ along the z-axis.

In the particular case of $\theta = 45°$ and $\varphi = 2\delta k_L$ the phase change along the y-axis will be equal to

$$\frac{\varphi}{4} = \frac{2}{4}\delta k_L = \frac{2}{4}\delta\frac{2\pi}{\lambda} = \delta\,\frac{\pi}{\lambda} \tag{13}$$

and along the z-axis it will be given by

$$\frac{\varphi}{2s} = \frac{1}{2}2\delta k_L = \delta\,\frac{2\pi}{\lambda}. \tag{14}$$

A phase shift of π corresponds to an increase of $\frac{1}{2\sqrt{2}}\lambda$ in physical space, hence:

$$\begin{aligned}\text{phase change} &\rightarrow \text{displacement}\\ \pi &\rightarrow \frac{1}{2\sqrt{2}}\lambda\\ \frac{\varphi}{4}=\delta\,\frac{\pi}{\lambda} &\rightarrow \frac{\delta}{\lambda}\frac{1}{2\sqrt{2}}\lambda=\frac{\delta}{2\sqrt{2}}\\ \frac{\varphi}{2}=\delta\,\frac{2\pi}{\lambda} &\rightarrow \frac{\delta}{\sqrt{2}}.\end{aligned}\tag{15}$$

Moving the translation stage a distance δ will displace the lattice by $\delta/2\sqrt{2}$ in the $\hat{\mathbf{z}}$-direction, and by $\delta/\sqrt{2}$ in the $-\hat{\mathbf{y}}$-direction.

Changing the optical path of a pair of beams

If the optical path of beam 1 and beam 2 (see Fig. 2) are increased by 2δ, the electric fields become

$$\begin{aligned}\mathbf{E}_1 &= E_0\hat{\mathbf{x}}\cos(\ \ k_\perp\, y - k_\parallel z+\varphi-\omega t)\\ \mathbf{E}_2 &= E_0\hat{\mathbf{x}}\cos(-k_\perp\, y - k_\parallel z+\varphi-\omega t).\end{aligned}\tag{16}$$

Because of the symmetry of the laser beam configuration, a prolongation of beam path 2 by $2\delta k_L$ results in a translation of the lattice by $-\varphi/2$ along the y-axis and by $-\varphi/4$ along the z-axis. Together with the effect of the prolongation of beam path 1 the total translation is $-\varphi/2$ along $\hat{\mathbf{z}}$, while the position along $\hat{\mathbf{y}}$ remains unchanged.

Changing the optical path of all beams

For a simultaneous change of all four lattice beams, the electrical fields become:

$$\begin{aligned}\mathbf{E}_1 &= E_0\hat{\mathbf{x}}\cos(\ \ k_\perp\, y - k_\parallel\, z+\varphi-\omega t)\\ \mathbf{E}_2 &= E_0\hat{\mathbf{x}}\cos(-k_\perp\, y - k_\parallel\, z+\varphi-\omega t)\\ \mathbf{E}_3 &= E_0\hat{\mathbf{y}}\cos(\ \ k_\perp\, x + k_\parallel\, z+\varphi-\omega t)\\ \mathbf{E}_4 &= E_0\hat{\mathbf{y}}\cos(-k_\perp\, x + k_\parallel\, z+\varphi-\omega t).\end{aligned}\tag{17}$$

Thus, the position of the lattice will remain unchanged. The phase φ is absorbed in the time-phase ωt. Thus, random phase jumps in the single laser beam, from which the fields $\mathbf{E}_i$ are derived, will not affect the optical lattice.

Overlapping two optical lattices

Here, we derive the travel range of the translation stages, which is necessary to change the relative position of the lattices by a given amount. The two laser wavelengths are $\lambda_\mathrm{B} = 852.355\,\mathrm{nm}$ and $\lambda_\mathrm{A} = 852.335\,\mathrm{nm}$. Assume, that at $z = 0$, the σ_+-sites of both lattices coincide. Along $\hat{\mathbf{z}}$, the standing waves of σ_+-light can be written as $\cos(2k_{\parallel_\mathrm{A}} z)$ and $\cos(2k_{\parallel_\mathrm{B}} z)$. After a certain distance z' the lattices will have dephased completely, so that:

$$\begin{aligned}\cos\left(2k_{\parallel_\mathrm{A}}\, z'\right) &= -\cos\left(2k_{\parallel_\mathrm{B}}\, z'\right)\\ \cos\left(\frac{4}{\sqrt{2}}\frac{\pi}{\lambda_\mathrm{A}}\, z'\right) &= \cos\left(\frac{4}{\sqrt{2}}\frac{\pi}{\lambda_\mathrm{B}}\, z'-\pi\right)\end{aligned}$$

comparing the arguments of the cosine functions we obtain

$$z' = \frac{\sqrt{2}}{4\left(\frac{1}{\lambda_\mathrm{B}}-\frac{1}{\lambda_\mathrm{A}}\right)} = 1.2869\ \mathrm{cm}.$$

In an analogous fashion the x- and y-directions can be treated:

$$\cos(k_{\perp_{\mathrm{A}}} y') = -\cos(k_{\perp_{\mathrm{B}}} y')$$

yielding:

$$y' = \frac{\sqrt{2}}{2\left(\frac{1}{\lambda_{\mathrm{B}}} - \frac{1}{\lambda_{\mathrm{A}}}\right)} = 2.5738 \text{ cm}.$$

In order to move an optical lattice along the y-axis by a given amount Δy, we have to increase the optical path of one beam by $2\sqrt{2}\Delta y$, *i.e.* we have to move the translation stage by $\sqrt{2}\Delta y$. Thus, to achieve a change in relative spatial phase by π, we need:

$$\delta' = \sqrt{2}\, y, \qquad \delta' = 3.6399 \text{ cm}.$$

For a translation along $\hat{\mathbf{z}}$, the same considerations lead to $\Delta z = z'$, which gives:

$$\delta' = \sqrt{2}\, z', \qquad \delta' = 1.8199 \text{ cm}.$$

Thus y' and z' are much larger than the diameter of the lattice ($\approx$0.05 cm). Thus, the relative spatial phase across the lattice volume can be considered as constant.

References

1. P. Jessen, I. Deutsch, Adv. At. Mol. Opt. Phys. **37**, 95 (1996)
2. G. Grynberg, C. Mennerat-Robilliard, Phys. Rep. **355**, 335 (2001)
3. D. Jaksch, H.-J. Briegel, J. Cirac, C. Gardiner, P. Zoller, Phys. Rev. Lett. **82**, 1975 (1999)
4. G. Brennen, C. Caves, P. Jessen, I. Deutsch, Phys. Rev. Lett. **82**, 1060 (1999)
5. A. Sørensen, K. Mølmer, Phys. Rev. Lett. **83**, 2274 (1999)
6. C. Monroe, Nature **416**, 238 (2002)
7. H. Ellmann, J. Jersblad, A. Kastberg, Phys. Rev. Lett. **90**, 053001 (2003)
8. P. Lett, R. Watts, C. Westbrook, W. Phillips, P. Gould, H. Metcalf, Phys. Rev. Lett. **61**, 169 (1988)
9. S. Dutta, N. Morrow, G. Raithel, Phys. Rev. A **62**, 035402 (2000)
10. H. Ellmann, J. Jersblad, A. Kastberg, Eur. Phys. J. D **13**, 379 (2001)
11. M. DePue, S. Winoto, D. Han, D. Weiss, Opt. Commun. **180**, 73 (2000)
12. F. Buchkremer, R. Dumke, H. Levsen, G. Birkl, W. Ertmer, Phys. Rev. Lett. **85**, 3121 (2000)
13. K. Eckert, J. Mompart, X.X. Yi, J. Schliemann, D. Bruß, M. Lewenstein, Phys. Rev. A **66**, 042317 (2002)
14. W.D. Phillips, C.I. Westbrook, Phys. Rev. Lett. **78**, 2676 (1997)
15. C. Cohen-Tannoudji, J. Dupont-Roc, G. Grynberg, *Atom-Photon Interactions* (Wiley, New York, 1992)
16. R. Dumke, M. Volk, T. Müther, F.B.J. Buchkremer, G. Birkl, W. Ertmer, Phys. Rev. Lett. **89**, 097903 (2002)
17. P. Verkerk, D.R. Meacher, A.B. Coates, J.-Y. Courtois, S. Guibal, B. Lounis, C. Salomon, G. Grynberg, Europhys. Lett. **26**, 171 (1994)
18. M.V. Klein, T.E. Furtak, *Optics* (John Wiley and Sons, New York, 1985)